Particle in Cell simulations on the effects of electrically biased grid to the plasma parameters

N. Jelić[1,2], Leon Kos[2]

[1]*Department of Theoretical Physics, University of Innsbruck, A-6020 Innsbruck, Austria*
[2]*LECAD Laboratory, Faculty of Mechanical Engineering, University of Ljubljana, SI-1000 Ljubljana, Slovenia*
E-mail: nikola.jelic@uibk.ac.at

Abstract

Recently Baalrud et al [Physics of Plasmas **14** *042109 (2007)] investigated a plasma under conditions of non-ambipolar flow, under special plasma confinement scenario where all electrons are lost to one boundary and all positive ions to another boundary. More generalized scenario of ambipolar flow to different boundaries was investigated by Jelic et al. [Contrib. Plasma Phys.* **43***/2 111 (2003)] via developing a self consistent theoretical model for calculating the plasma potential, plasma density and electron temperature. Both approaches rely on so called zero dimensional approximation. Since the problem of ambipolar flow is an important one in space, laboratory and fusion plasmas as well as in Langmuir probe diagnostics, we employ a one-dimensional Particle in Cell (PIC) code to simulate the plasma behavior in the presence of an electrically biased object in higher dimensionality. Simulated results agree well with theoretical predictions and experimental results, but may be considered as more reliable ones.*

1 Introduction

The possibility to control the plasma flow at local boundaries, rather than to the walls, via using additional biased electrodes immersed in plasmas, has been recognized for a long time in laboratory technology-oriented and fusion-related plasmas. In hot-filament discharges like double plasma devices (DPDs), as well as in simplified (single) or extended (triple) devices, the effects of mechanical and electrical supports and additional electrodes, probes, additional wire grids for electron heating, electrostatic confinement grids, as well as the filament cathode arrangements, the ionizing electron beams, the local magnetic cusp installations at the plasma boundaries, constant external magnetic fields, etc., were studied via using both theoretical and experimental method. There is also a long history of electrostatic confinement of plasmas in spherical geometries as designed for nuclear reaction applications where various electrically biased objects in combinations with other local fields and structures take role. An electron absorbing boundary can be represented also by a Double Layer (DL) structures instead of a solid surface. Such DL formations of anode type (also known as "fireball" or "fire-rod") were studied in detail in the past (see e.g., recent work of Baalrud et al from 2009 [1]. As a rough common conclusion it turns out that there are at least three important properties of the *local* plasma boundary which either influence or completely determine the plasma parameters, namely (i) the *effective* surface (ii) geometry of surface and (iii) the electric bias of surface.

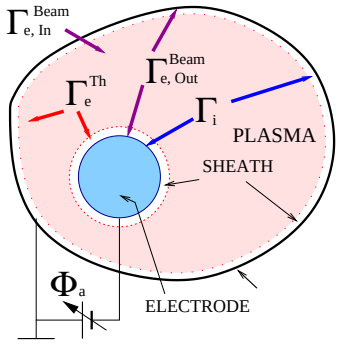

Figure 1: Symbolic picture of a plasma chamber with immersed anode of variable size

Up to date self-consistent theoretical considerations of the influence of electrically biased objects are based on so called "two-point model", known also as a "zero-dimensional approximation" applied to a rather general geometry as symbolically presented in Fig. 1. The plasma parameters are calculated at a point far from all boundaries. The case with vanishing electrode size [2] yield the "similarity rule" based on which the plasma parameters can be calculated as a function of the single quantity named as the "discharge efficiency" $e\Phi_p$ defined via expression:

$$e\Phi_p \equiv \frac{1}{n_a \vartheta \frac{V}{A}, \sqrt{\frac{m_i}{m_e}}}, \qquad (1)$$

where e is the elementary charge, m_i and m_e are the ion and electron masses respectively, V is the plasma volume and A is the total plasma surface bounding volume V, n_a is the density of the background gas and ϑ a quantity related to the semi-empiric expression for the ionization cross-section expressed in the form

$$\sigma_i(K) = \vartheta \frac{9(e\Phi_I)^2(K - e\Phi_I)}{, K(K + 8e\Phi_I)} \qquad (2)$$

with K the kinetic energy of electrons and $e\Phi_I$ the first ionization level, ϑ a characteristic constant of the kind of

gas used. The values of ϑ calculated on precise results of cross-section measurements done by Stefan et al and Stefan and Märk [3]. For convenience the discharge efficiency is normalized as

$$\frac{e\Phi_I}{e\Phi_p} \equiv n_a \vartheta e\Phi_I \frac{V}{A}\sqrt{\frac{m_i}{m_e}}\,, \qquad (3)$$

which quantity has been shown [2] to scale as ν_I/ν_L with $\nu_{I,L}$ the characteristic frequencies of plasma volume gains and surface losses. Taking into account the presence of a positively biased (electron absorbing) electrode immersed in plasma, the complete problem has been solved via calculating mentioned plasma parameters consistently, as functions of the electrode bias and with variable electrode size [4]. Here we employ the model of Baalrud et al for calculating the plasma potential as follows, however, with relaxed boundary conditions.

For the *monotonic ion sheath* the current continuity follows from equality of ion and electron currents to the anode and wall (with areas A_a and A_w respectively and with respective fluxes Γ_i and Γ_e), according to relation $I_i = I_e$ where $I_i = \Gamma_i A_e + \Gamma_i A_w =$ and $I_e = \Gamma_{e,Th} = A_e \exp(V_a - \Phi) + A_w \exp(e\Phi)$, with Φ the bulk plasma potential far from the anode and with the anode bias voltage V_a. Having in mind that $\Gamma_i = n_0\alpha\sqrt{kT_e/m_i}$ (where α is a function which can be approximated by a constant of the order of unity) and that the electron current is given

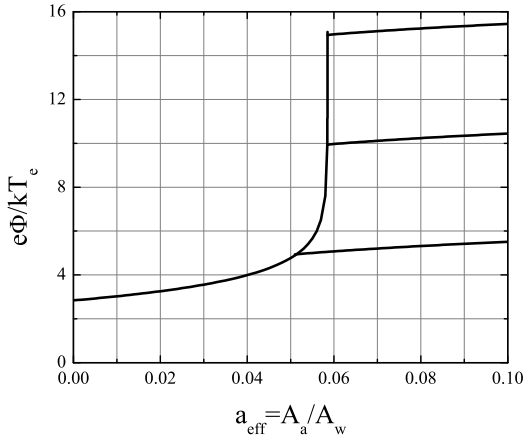

Figure 2: Theoretical plasma potential as a function of the anode size, obtained for anode voltages $V_a = 5,\ 10,\ 15\ kT_e$

by $\Gamma_e = n_0\sqrt{kT_e/2\pi m_e}$ the solution of last equality yields a first branch of solution for the plasma potential as measured to the ground potential $\Phi_w = 0$ for the *electron reach sheath* in the form:

$$\frac{e\Phi_{up}}{kT_e} = -\ln\left[\alpha\sqrt{\frac{2\pi m_e}{m_i}} - a\right] \qquad (4)$$

Second branch of solution, i.e., for the case of monotonic *ion-reach sheath* is:

$$\frac{e\Phi_{dn}}{kT_e} = -\ln\left[\alpha\sqrt{\frac{2\pi m_e}{m_i}}\,\frac{1+a}{1+a\exp(e\Phi_a/kT_e)}\right] \qquad (5)$$

where $a \equiv A_a/A_w \simeq A_a/(A_w + A_a)$ is introduced for shortness. Superscript "up" means that the plasma potential is above the anode potential and superscript "dn" is the opposite case. The intersection point (superscript "cr") of the two branches is simply

$$a_{cr} = \alpha\sqrt{\frac{2\pi m_e}{m_i}} + \left(1 + \alpha\sqrt{\frac{2\pi m_e}{m_i}}\right)\exp(\frac{-e\Phi_a}{kT_e}) \qquad (6)$$

Thus we obtain two branches of solution which are presented in Fig. 2 with $a_{cr} = \sqrt{2\pi m_e/m_i}$, for $\alpha = 1$.

2 Particle in Cell Simulations

Increased computational resources promise efficient employment of kinetic simulations known as Particle in Cell (PIC) simulations (see e.g., [5, 6] and references therein) which, in principle, can resolve plasma behavior at any local point including the regions of strong electric fields, like plasma sheaths and double layers. Te code is electromagnetic but for the present purposes we take into account only electric field. The main loop of the code starts from an initially empty, or filled by ions and electrons distributed randomly in configuration-velocity space (phase-space) computational domain in a prescribed electric field, and (1) solves the Newton equations of motion either for each particle (or for so-called super-particles – clusters of particles) via integrating them during properly chosen, enough short, time-step Δt. Then (2) a new particle balance is established where particle loss/gain at boundaries have been taken into account. and new positions and velocities of all new and old particles are found are found. follows (3) the interpolation of particle sources to grid and (4) integration of field equations. . After (5) interpolating new fields to particles the main loop is finished. Monte Carlo Collision method (6) for binary collisions is available between steps (2) and (3). The computational power, however, is still not sufficient for many scenarios of interest, i.e., for both complicated geometries and demanding physical scenarios. This restriction can be sometimes solved via using proper simplifications. Here we employ 1D-3v (one-dimensional in space and three-dimensional in velocity coordinate) XPDP1 code [6] for attacking a quasi-3D case as in Fig. 1.

For the present purpose we adapt the code for solving one half of the system as sketched in Fig.3. We employ fine biased grids (e.g., G_1 and G_2) with adjustable bias voltages for achieving the desired degree of reflection (transparency) from either to another chamber. This is similar to the arrangement of a so called double plasma device (DPD). One can control the ion and electron fluxes and the plasma potentials in both sides of DPD's, i.e., to obtain a variety of potential profiles. Via choosing proper transmission degrees for ions and electrons we simulate an effective electrode size biased at a proper potential. With this arrangement the plasma potential can be held bellow the bias voltage of the boundary (the grid). If both grids G_1 and G_2 are biased at the same arbitrary potential, and the distance between grids is bellow the Debye length $\lambda_D = \sqrt{\epsilon_0 kT_e/ne^2}$, a high transparency corresponds to the of a small electrode, while high reflectivity corresponds to an electrically floating wall.

The length of computational region is varied between 3 and 6 cm and the number of equidistant grid cells in the

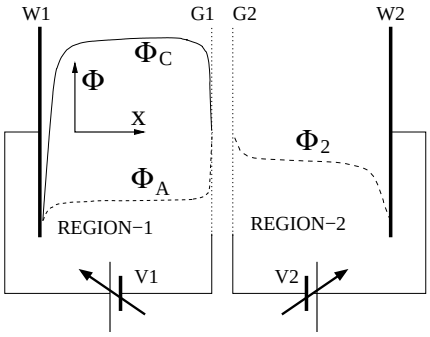

Figure 3: Our basic diagram illustrating employment of biased grids (e.g., G_1 and G_2) for controlling the plasma potentials in both sides of a DPD's, i.e., for obtaining a variety of profiles via applying proper grid's biases. In this work we deal with an ideally symmetric discharge with positively biased grids at the equal potential with variable grid transparency starting from 1 and decreasing to zero for obtaining critical value a_{cr} for which the plasma parameters are dominating by the biased object.

system has been typically several thousand in order to obtain the length of one cell from $2 \times 10^{-5}\, m$ to $1.25 \times 10^{-6}\, m$. For one time step we take typically 5×10^{-11} s. The electron temperature is kept in a wide in the range $1eV$ - $100eV$ but the ionization neither with beam nor with thermal electrons has been taken into account. The production rate of charged particles has been set to such a strength that in the steady state the density of charged particles in the middle of the system is ranging from approximately $1 \times 10^{14} m^{-3}$ - $1 \times 10^{18} m^{-3}$. In this way, i.e., by varying either n_e or T_e the Debye length, has been varied for more than two orders of magnitude. Typically the Debye length is kept much smaller than the system length, i.e., being no more than some percents of it. although the cases without real quasi-neutrality (plasma diodes) were obtained as well. Typically there are 4 - 5 cells per Debye length. On the other hand we kept about several tens of calculation time steps per electron plasma period which is typically of the order of several GHz. The number of physical particles per computer particle (super particle) was also varied. The number of cells per Debye length is kept between 4 and 5 and several tens of time steps per electron plasma period are maintained. Initially the system is empty. The steady state is typically reached after about 5×10^{-5} physical seconds. Computer time for reaching this steady state, however, was 10^{11} - 10^{12} longer. In order to get relatively smooth curves all the results have been averaged over a large number of times steps. The period of time steps also defines spectral resolution of the amplitude spectra of the plasma potential oscillations. With increased densities the procedure becomes considerably more time-consuming.

3 Results

Firstly, we show results of a series of simulations with electrode biased at $10\ V$ with respect to with grounded wall performed with the electron temperature $kT_e = 1\, eV$. The profiles are obtained for increased electrode size. The spatial profiles of the plasma potential and the electron

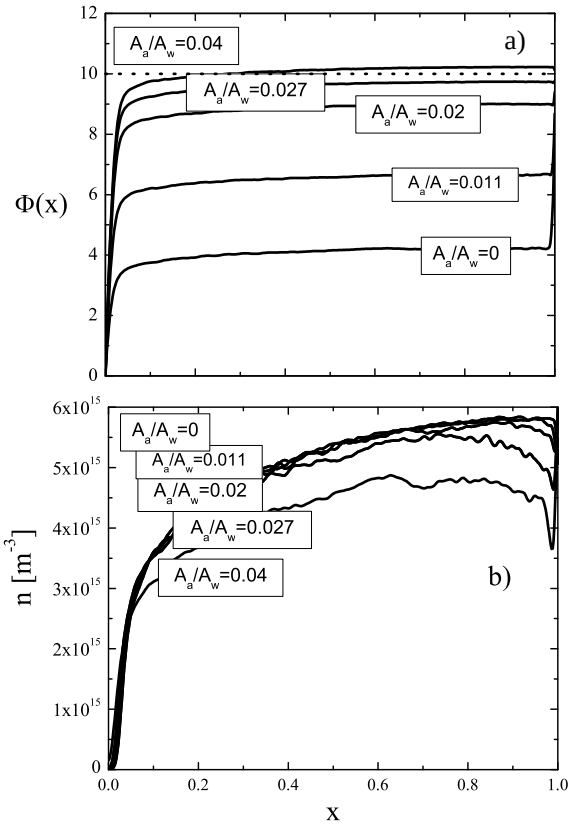

Figure 4: Potential profiles (a) and density profiles as simulated for several anode sizes with fixed anode voltage $\Phi = 10\ V$ and $kT_e = 1\ eV$

density were recorded as shown in Fig. 4. The critical anode surface is expected to be close to reduced model in which we predict the value defined by $A_a/A_w = a_{cr}$. It is obvious from Fig. 4 that for very small anode surfaces (high grid transparency) there is an electron reach plasma sheath formed near the grid (anode) while for enough large (but still relatively small) collecting surface this behavior in the vicinity the surface, i.e., at both sides the sheaths become the ion-reach. At the same time the density which correspond to potential profiles slightly depends on the anode (grid) bias.

In Fig. 5 we show the normalized plasma potentials in the middle of the system obtained from PIC simulations in comparison with the theoretical predictions, as functions of the anode effective surface, for Hydrogen and Argon, and found that the two type of results agree with each other qualitatively well. For further direct comparison of PIC results with theoretical and experimental ones we have available set of all data for Argon. In Fig. 6 we plot these data as obtained for mentioned pressure $0.04/Pa$ in the full-length DP machine. Inspections of the value A_a/A_w where the anode potential equals the plasma potential give an estimation of $A_a/A_w \simeq 0.013$ for both PIC results and self consistent theoretical calculations whereas for experimental results $A_a/A_w \simeq 0.02$. Lets recall in mind that the last result is nearest to the value $A_a/A_w \simeq 0.0187$ obtained for Argon obtained with strongly simplified assumption. It is difficult to say whether the famous factor $\alpha \simeq 0.6$ proposed by Baalrud et al., should be taken into account, since this value would

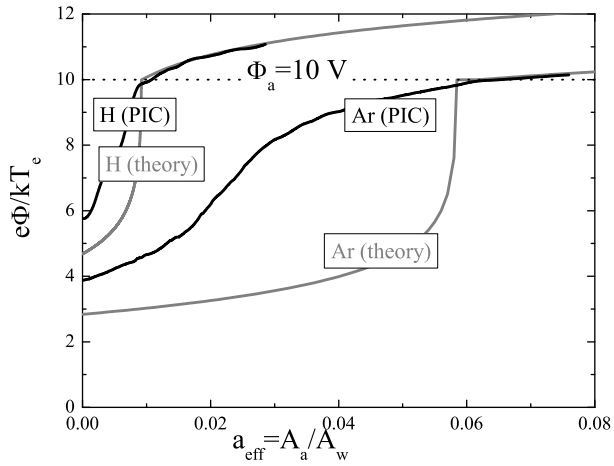

Figure 5: Normalized plasma potentials in the middle of the system obtained from PIC simulations in comparison with the theoretical predictions, as functions of the anode effective surface, for Hydrogen and Argon.

lead to considerable discrepancy between theory and PIC simulation results on one side and experimental measurements on another side. On the other hand our choice $\alpha = 1$ is also under the question for simple reason that in the present work it was not calculated self-consistently as $\alpha = \alpha_1\alpha_2\alpha_3$ but just taken as an estimation. In this light the good agreement of the value $A_a/A_w \simeq 0.013$ obtained in both PIC and theoretical prediction might be regarded as surprisingly good. Having in mind that all

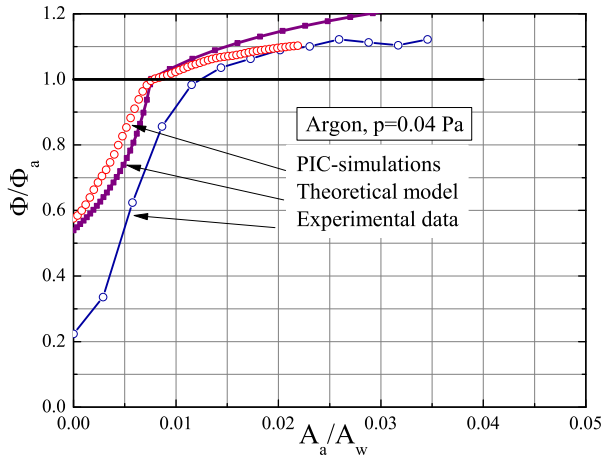

Figure 6: Re-normalized plasma potential for Argon plasma, in the middle of the discharge as obtained from PIC simulations, in comparison experiments and theoretical results

the three kind of results are obtained under rather various assumption's and technical solutions the similarity of the results seems to yield an estimation of what means "large" and small positively biased electrode. It is obvious, that the plasma potential is, in any model, considerably perturbed by small biased object. This holds even in the case $A_a/A_w \to 0$. From this point of view a positively biased electrode is always "large". A jump occurs near a value, which is related to the boundary conditions via a week function α, which is possible to approximate with a constant near unity, to be determined in future self-consistently, for any particular discharge scenario separately.

4 Summary

We present the results of employing Particle in Cell numerical simulation for investigating possibilities to control the plasma parameters by immersing a small positively electrode biased at the highly positive voltage (with $e\Phi_a \gg kT_e$). There are some quantitative discrepancies between theoretical, experimental and PIC simulation results presented here. Namely, the theoretical model is based on *zero-dimensional* geometry with a specified mechanism of ionization originating from beam atom impacts and thermal ionization. The experimental method is essentially *three-dimensional* and many processes like e.g., charge exchange which were not taken into account in theoretical model take role. In addition, and most important in experiment is the fact that the effective surface for plasma losses at the wall is just estimated and it is not a simple task to make very precise calculation on the actual plasma losses area. On the other hand, the present PIC model also simplified one regarding the physical processes taken into account in simulations. Simulations are performed in *one-dimensional* geometry and are based on a free-fall model of collisionless discharge which might be regarded as an over-simplification when applied to an arbitrary 3D geometry. Having in mind these facts we may conclude that the agreement between the three kind of method is better than it may be expected.

Acknowledgments

This work was supported by the Austrian Academy of Sciences and by the Austrian Science Fund (FWF) under project P19333-N16.

References

[1] S. D. Baalrud, N. Hershkowitz, and B. Longmier, "Global nonambipolar flow: Plasma confinement where all electrons are lost to one boundary and all positive ions to another boundary," *Phys. Plasmas*, vol. 14, no. 4, p. 042109, 2007.

[2] N. Jelić, S. Kuhn, and R. Schrittwieser, "Similarity rules for collisionless hot-filament discharges," *Contrib. Plasm. Phys.*, vol. 43, no. 2, pp. 94–110, 2003.

[3] K. Stephan, H. Helm, and T. D. Märk, "Mass spectrometric determination of partial electron impact ionization cross sections of he, ne, ar and kr from threshold up to 180 ev," *J. Chem. Phys.*, vol. 73, no. 8, pp. 3763–3778, 1980.

[4] N. Jelić, R. Schrittwieser, and S. Kuhn, "Effects of electron-absorbing boundaries on the plasma parameters of a hot-filament discharge," *Contrib. Plasm. Phys.*, vol. 43, no. 2, pp. 111–121, 2003.

[5] C. Birdsall, "Particle-in-cell charged-particle simulations, plus monte carlo collisions with neutral atoms, PIC-MCC," *Plasma Science, IEEE Transactions on*, vol. 19, pp. 65 –85, apr 1991.

[6] J. P. Verboncoeur, M. V. Alves, V. Vahedi, and C. K. Birdsall, "Simultaneous potential and circuit solution for 1D bounded plasma particle simulation codes," *J. Comput. Phys.*, vol. 104, no. 2, pp. 321–328, 1993.